Effect of curing conditions after compaction on the strength development of soils treated with paper sludge ash-based stabilizer

Navila Tabassum, Hayano Kimitoshi
Department of Urban Innovation-Yokohama National University, Yokohama, Kanagawa, Japan
Yamauchi Hiromoto
domi Environmental Solutions,Japan

ABSTRACT
Construction generated soils have been recycled worldwide in construction projects for decades. It is sometimes necessary to treat construction generated soils by the addition of stabilizing agents such as cement or quicklime to improve the characteristics, which sometimes leads to financial and environmental problems. To overcome these issues, studies on the use of sustainable materials generated from industrial processes have been conducted. Soil stabilization using paper sludge ash-based stabilizers (PSAS) has been developed as one of the attempts to use sustainable materials generated from industrial processes in construction works. PSAS can be produced by insolubilizing heavy metals in original paper sludge (PS) ash particles, which is a waste generated by the incineration of PS discharged from paper mills. The surface of the PSAS particles is porous having many voids and complex irregularities. Because of these characters, PSAS can absorb and retain extra water in soils immediately when it is mixed with the construction soil. Moreover, recent studies related with PSAS reported that the water absorption and retention performance of PSAS increases with curing period. This is because PSAS create a hydration reaction when combined with water, although the reaction is not as strong as that of cement. Taking advantage of the characteristic, construction-generated soils with high water contents, treated with PSAS can be used as filling or embankment materials. When PSAS treated soil is used as river embankment material, it is expected that dry and wet cycles may have some effects on strength development of PSAS treated soil. This study aims to investigate the effects of dry and wet cycles on the strength development characteristics of PSAS-treated soils. For comparison, same investigation was conducted on the soils treated with blast furnace cement type B (BFCB).

RÉSUMÉ
Les sols générés par la construction sont recyclés dans le monde entier dans des projets de construction depuis des décennies. Il est parfois nécessaire de traiter les sols générés par la construction par l'ajout d'agents stabilisants tels que le ciment ou la chaux vive pour en améliorer les caractéristiques, ce qui entraîne parfois des problèmes financiers et environnementaux. Pour surmonter ces problèmes, des études sur l'utilisation de matériaux durables issus de procédés industriels ont été menées. La stabilisation des sols à l'aide de stabilisants à base de cendres de boues de papier (PSAS) a été développée comme l'une des tentatives d'utilisation de matériaux durables générés à partir de processus industriels dans les travaux de construction. Le PSAS peut être produit en insolubilisant les métaux lourds dans les particules de cendres de la boue de papier (PS) d'origine, qui est un déchet généré par l'incinération du PS rejeté par les papeteries. des études récentes liées au PSAS ont rapporté que les performances d'absorption et de rétention d'eau du PSAS augmentent avec la période de durcissement. En effet, les PSAS créent une réaction d'hydratation lorsqu'ils sont combinés avec de l'eau, bien que la réaction ne soit pas aussi forte que celle du ciment. Profitant des sols caractéristiques, générés par la construction et à forte teneur en eau, traités avec PSAS peuvent être utilisés comme matériaux de remplissage ou de remblai. Cette étude vise à étudier les effets des cycles secs et humides sur les caractéristiques de développement de la résistance des sols traités au PSAS. A titre de comparaison, la même enquête a été menée sur les sols traités avec du ciment de haut fourneau de type B (BFCB)

1. INTRODUCTION

In Japan, the surplus soil generated from construction, excluding construction waste sludge (which is regulated as industrial waste), is called construction-generated soil. Such construction-generated soils have been recycled in construction projects for many decades, not only in Japan but worldwide. (Kitazume and Hayano, 2003, 2007; Siham et al., 2008). However, construction-generated soils often have negative characteristics for use as geomaterials in construction projects. Therefore, construction-generated soils are occasionally treated by adding stabilizing agents such as cement or quicklime to improve their characteristics; however, this can result in financial and environmental problems (Dong et al, 2011, Imai et al., 2020, Trung et al., 2021, Inasaka et al., 2021, Djandjieme

et al., 2022). To overcome these problems, studies have been conducted on the use of sustainable materials generated from industrial processes, such as coal ash steel slag, concrete sludge, biomass ash, sewage sludge ash, and fly ash.

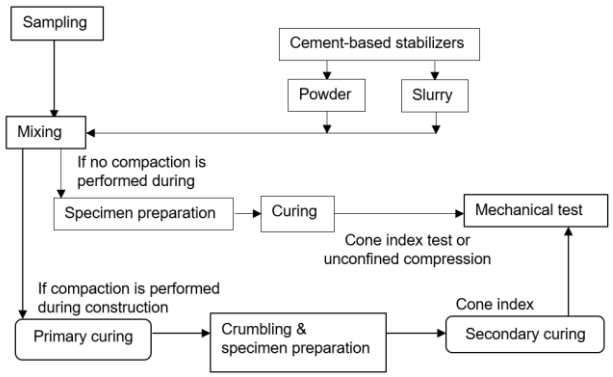

Figure 1 Conventional flow of laboratory mixture design for treating construction-generated soil with cement-based stabilizers (revised from Public Works Research Institute, 2013)

Soil stabilization using paper sludge ash-based stabilizers (PSASs) has also been developed, PSASs can be produced by insolubilizing heavy metals in original paper sludge (PS) ash particles, i.e., the wastes generated by the incineration of the PS discharged from paper mills. The surface shape of a PS ash particle has a porous structure with many complex irregularities and voids. Scholars have reported that the water absorption and retention performance of PSASs increase with curing (Phan et al., 2021, Watanabe et al., 2021). This is because a PSAS is expected to create a hydration reaction when combined with water, although the reaction is not as strong as that of cement.

Figure 1 shows the conventional flow of the laboratory mixture design for treating construction-generated soil with cement-based stabilizers (Public Works Research Institute, 2013) Generally, if no compaction is performed during construction, the specimens are cured after being prepared by mixing the soil with the cement-based stabilizer. Consequently, mechanical tests such as cone index tests or unconfined compression tests are conducted on the specimens. However, if compaction is performed during construction, the primary curing is conducted on the soil–cement mixture, and subsequently, the mixture is crumbled. Thereafter, the crumbled mixture is immediately compacted followed by secondary curing. The compacted specimens are subjected to the mechanical tests (such as cone index tests) after the second curing step. Previous studies have reported that the strength characteristics of construction-generated soils treated with cement or lime are strongly affected by the secondary curing conditions (Miyashita et al., 2019). These findings suggest that the strengths of PSAS-treated soils are affected by these conditions. However, this problem has not been investigated in detail.

Therefore, this study investigated the effects of the secondary curing conditions on strength characteristics of PSAS-treated soils using two types of PSASs with different water absorption and retention performances. For comparison, the same investigation was conducted on soils treated with blast furnace cement type B (BFCB).

2. METERIALS USED FOR SAMPLE PREPARATION

Ao clay, which is commercially available in Japan, was used in this study to represent the construction-generated soil. The clay is categorized into CL (clay low liquid limit) according to the Unified Soil Classification System. The physical properties were as follows: particle density, ρ_s = 2.716 g/cm3, liquid limit wL = 40.7%, plastic limit wp =23.7%, and plasticity index Ip =17.0. The particle size distribution (PSD) of Ao clay, as obtained from the soil particle size test method according to the Japanese Geotechnical Society (JGS) Standard 0131, is shown in Figure 2. Two types of PSASs and a BFCB were used to treat the Ao clay. The two PSASs were denoted as PSAS-N and PSAS-R, and both were produced by insolubilizing heavy metals in the original PS ash particles.

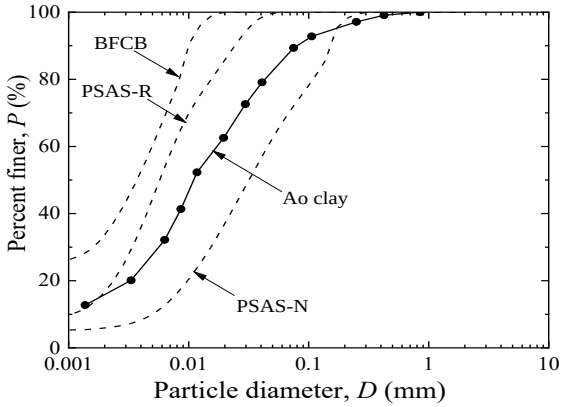

Figure 2 Particle size distributions of Ao clay, PSAS-N, PSAS-R, and BFCB

However, the type of original PS ash used differed between PSAS-N and PSAS-R. The ρ_s of PSAS-N and PSAS-R were 2.603 and 2.840 g/cm^3, respectively, and that of BFCB was 3.04 g/cm^3. Figure 2 also shows the PSDs of two PSASs (PSAS-N and PSAS-R) and BFCB. Owing to their hydration progress, the soil particle size test according to JGS 0131 was not conducted on PSAS-N, PSAS-R, and BFCB. Instead, the PSDs of the two PSASs and BFCB were obtained using a laser diffraction-type PSD-measuring device that used ethanol as the solvent instead of an aqueous solution. The particle size of PSAS-R was smaller than that of PSAS-N. Table 1 lists the chemical compositions of PSAS-N, PSAS-R, and BFCB. The calcium oxide (CaO) content accounts for 63.89% and 72.49% of PSAS-N and PSAS-R, respectively, whereas CaO content accounts for 65.57% of the BFCB. As the amounts of CaO were similar among the three stabilizers, the two PSASs were expected to undergo hydration reactions when combined with water, although the reactions were not the same as those of the BFCB. This was because when the BFCB was mixed with the

construction-generated soil, the strength development of the treated soils occurred through a hydration reaction, such as a pozzolanic reaction. In contrast, for the two PSASs, the excess water in the construction-generated soil was physically absorbed by the porous structures of the PS ash particles and subsequently chemically used to generate hydrates such as ettringite during curing (Kawai et al., 2018). As described in the previous section, PSASs have recently attracted interest as mud stabilizers owing to their water absorption and retention performance. However, the water absorption and retention performances of PSASs differ owing to the differences in the particle size and chemical composition of each PSAS (Mochizuki et al., 2004). Therefore, it is important to evaluate the water absorption and retention performance of each type of PSAS. Based on this, Phan et al. (2021) recently developed a new testing method for investigating the water absorption and retention performances of PSASs. In this study, the water absorption and retention performances of PSAS-N and PSAS-R were investigated using this method.

Table 1 Chemical component compositions of PSASs (PSAS-N, PSAS-R) and BFCB (% mass ratio)

(a) PSAS-N

CaO	SiO_2	Al_2O_3	SO_3	Fe_2O_4	TiO_2	MgO	P_2O_5	others
63.89	13.55	6.89	6.06	3.27	2.99	1.31	0.95	1.09

(b) PSAS-R

CaO	SiO_2	Al_2O_3	SO_3	Fe_2O_4	TiO_2	MgO	P_2O_5	others
72.49	11.42	8.43	3.07	1.01	1.34	1.48	0.55	0.23

(c) BFCB

CaO	SiO_2	Al_2O_3	SO_3	Fe_2O_4	MgO	TiO_2	MnO	P_2O_5	others
65.57	19.07	5.26	3.98	2.91	1.98	0.60	0.17	0.23	0.23

Figure 3 illustrates the experimental principle. Each type of PSAS was first soaked in distilled water using a PSAS/water ratio of 0.25, and was cured under sealed conditions for predetermined periods before being transferred to a sieve. The curing period varied from 10 min to 72 h. Subsequently, a three-dimensional vibration produced by an electromagnetic sieve shaker was applied to the PSAS in a stainless 53-μm sieve to separate the PSAS particles that absorbed and retained water from the free water in the PSAS solution (Figure 3). The three-dimensional movement was a circular motion superimposing a vertical throwing motion, and the amplitude was defined as the total lifting height of the test sieve. Owing to the impact of the vibration, the PSAS particles moved close together and were retained on the sieve, whereas the free water passed through. The water content of the PSAS particles retained on the stainless-steel sieve was then measured.

Figure 4 shows the test results for PSAS-N and PSAS-R. We observed that the water content of the two PSASs increased with the curing time. However, the rate of increase gradually decreased as the curing time increased. According to Phan et al. (2021), to eliminate the amount of free water in the voids trapped by the suction, the difference between the measured water content of the PSAS and that of sand or glass beads (= 22%) could be evaluated as the actual water absorption and retention ratio (W_{ab}) of the PSASs. Here, W_{ab} was defined as the ratio of the mass of the absorbed and retained water to the dry mass of the PSAS. As shown in Table 2, the W_{ab} values were estimated for PSAS-N and PSAS-R after 45 min, 24 h, and 72 h of curing. The results shown in Table 2 indicate that PSAS-R had higher water absorption and retention performance from the early stage than PSAS-N. This may be attributed to the differences in the particle size and CaO content between PSAS-N and PSAS-R, as mentioned earlier.

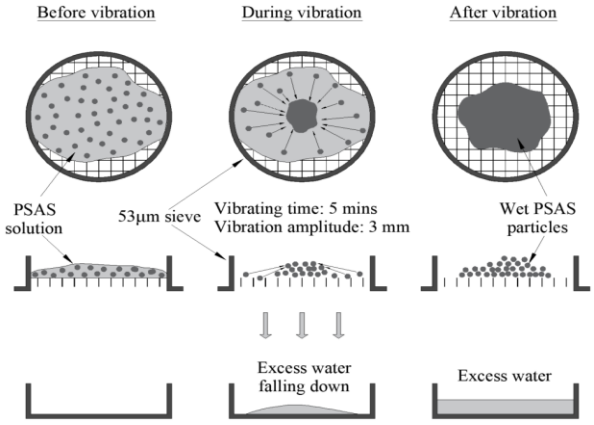

Figure 3 Experimental principle to determine the water absorption and retention performance of PSASs (Phan et al., 2021)

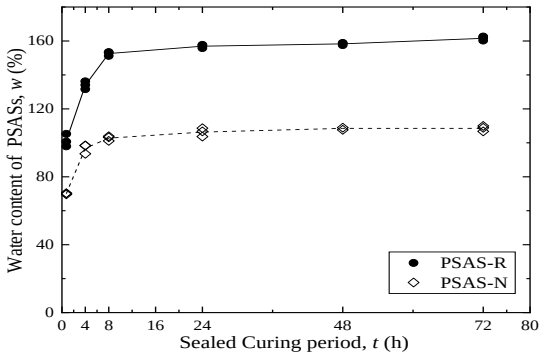

Figure 4 Change in water content of the PSAS-N and PSAS-R with the sealed curing period derived from water absorption and retention evaluation tests

Table 2 Estimated water absorption and retention ratio (W_{ab}) of the two PSASs

Water absorption and retention ratio, W_{ab} (%)	Sealed curing period of the PSAS		
	45 min	24 h	72 h
PSAS-N	54.2	85.6	85.6
PSAS-R	86.4	137.1	137.3

3. SAMPLE PREPARATION & TESTING METHOD

Figure 5 shows the process flow from sample preparation through sample preparation, compaction, and secondary

curing to the cone index tests. As shown in the figure, PSAS-treated samples (PSAS-N-treated and PSAS-R-treated samples) and BFCB-treated samples were prepared. Table 3 summarizes the mixture ratios of the treated samples. The initial water content of Ao clay was adjusted to w = 40.7%, i.e., the same as the liquid limit (w_L). Subsequently, to prepare the PSAS-treated samples, we mixed PSAS-N or the PSAS-R with Ao clay at 20% for the dry mass ratio, whereas for the BFCB-treated samples, the BFCB was mixed with Ao clay at 6%. Each sample was mixed for 10 min using a compact kitchen mixer in a vessel (diameter: 220 mm, depth: 190 mm). A paddle (135-mm wide and 115-mm high) was used to agitate each sample at 105 rpm.

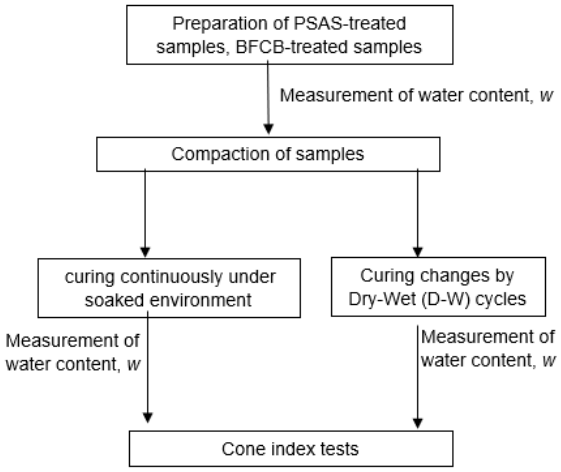

Figure 5 Flow of the process from sample preparation to cone index tests

As shown in Figure 5, Immediately after preparing the samples, the water content (*w)* was measured, and samples were compacted into molds following the JGS standard JIS A 1210. Each sample was placed in a 10-cm mold by first dividing the sample into three equal layers; then, each layer was sequentially added to the mold and compacted 25 times by dropping a 2.5-kg hammer from a height of 30 cm.

Table 3 Mixture ratios for PSAS-treated and BFCB-treated samples

Sample type	Initial water content of Ao clay, w_0 (%)	Addition ratio of PSAS-N or PSAS-R, A_{PS} (%)	Addition ratio of BFCB, A_{BFCB} (%)
PSAS-treated samples (PSAS-N-treated samples, PSAS-R-treated samples)	40.7 ($w_0 = w_L$)	20	0
BFCB-treated samples		0	6

For the secondary curing, two different conditions were used. Some molds containing the treated samples were soaked in water. The entire mold was immersed in water and cured such that the top surface of the specimen was in direct contact with the water at room temperature. Other molds containing treated sample, went through Dry and wet (D-W) cycles. For each D-W cycle, sample was kept 2 days at oven at 40º C temperature and 1 day the entire mold was immersed in water at room temperature (Figure 6). In each cycle, after drying and wetting, the weight of mold is measured and water content (*w*) in each drying and wetting process is calculated. Figure 7 shows the continuous change in water content due to repeated D-W cycles in the changes PSAS-N-treated, PSAS-R-treated BFCB-treated samples. Figure 8 shows the continuous change in degree of saturation, (s_r) due to repeated D-W cycles in the changes PSAS-N-treated, PSAS-R-treated BFCB-treated samples using *w*.

Figure 6 Samples subjected to Dry-Wet (D-W) cycles

Figure 9 demonstrates the change in appearance of the PSAS-N-treated, PSAS-R-treated BFCB-treated samples after 4th D-W cycles. After the required secondary curing period, cone index tests were conducted according to JGS 0716. Various curing periods and environment were used, as listed in Table 4. The test case names in Table 4 indicate the type of stabilizer, type and duration of curing. For example, PSN-7 is PSAS-N treated sample with a total curing period of 7 days under the soaked environment, and PSR-Cy-3 is PSAS-R treated sample with 3 D-W cycles with a total curing period of 9 days.

4 STRENGTH DEVELOPEMENT

After the required curing for different specimen, cone index tests were conducted on samples continuously soaked into water and samples going through continuous D-W cycles. Figure 10 shows the relationships between the cone index (q_c) and total curing period (t) of the PSAS-N-treated and PSAS-R-treated samples continuously soaked into water. The relationship between the BFCB-treated samples continuously soaked into water is also shown in the figure. The PSAS-R-treated samples exhibited a significant increase in strength in the early stage, whereas the PSAS-N-treated samples had a relatively low strength in the early stage and gradually increased in strength. The difference observed in q_c in Figure 9 partially harmonized with the difference in water absorption and retention ratio (W_{ab}) between PSAS-N and PSAS-R (Table 2). However, as shown in Figure 4, the water absorption and retention performance of both PSAS-N and PSAS-R hardly

increased after 24 h, whereas as shown in Figure 9, the q_c of the treated samples increased after 24 h. Although details of the reason for this gap should be studied further, the reaction between the PSASs and Ao clay might contribute to the increase in q_c. Additionally, Figure 9 shows that the BFCB-treated samples exhibited intermediate strengths between those of the PSAS-R-treated and PSAS-N-treated samples.

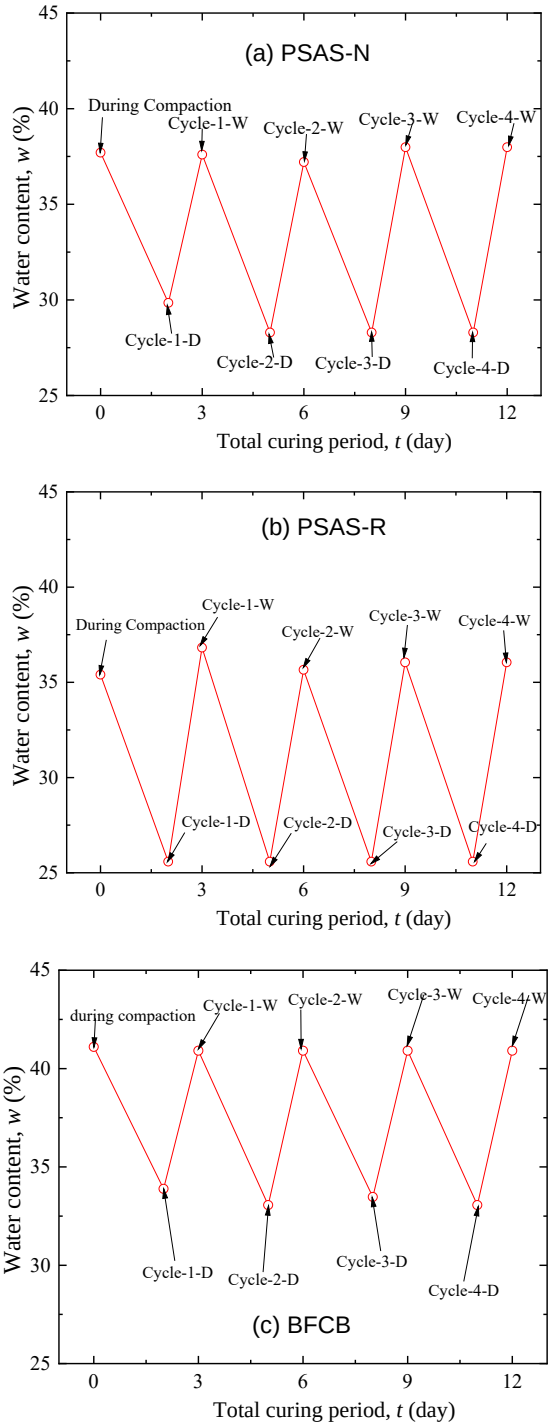

Figure 7 Change in water content in due to repeated D-W cycle.

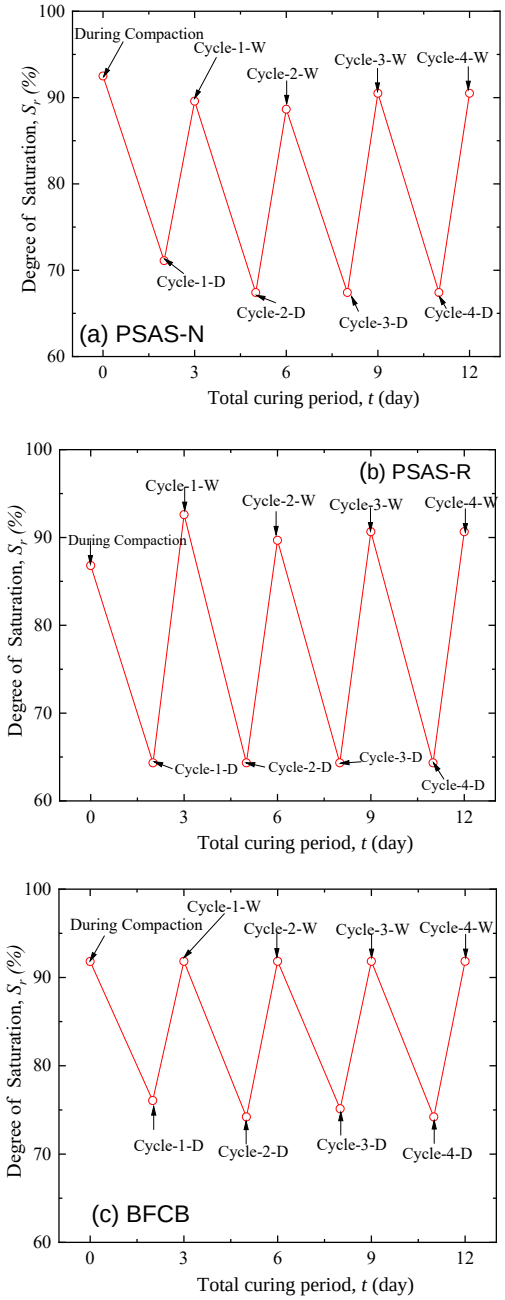

Figure 8 Change in Degree of saturation, (s_r) due to repeated D-W cycle

However, note that the addition ratio of BFCB (A_{BFCB}) was different from that of PSAS-R and PSAS-N (A_{PS}). Figure 11 shows the relationship between q_c and t for the samples continuously soaked into water for required time period and samples going through continuous D-W cycles . Figs. (a), (b), and (c) show the relationships of the PSAS-N-treated, PSAS-R-treated, and BFCB-treated samples, respectively. As shown in the figures, regardless of the difference in the

curing conditions, q_c increased with t; Focusing on the q_c of the samples, Figure 11 shows that the strength development differed depending on the type of stabilizer and curing period. Regardless of the type of stabilizer the q_c value of samples going through continuous D-W cycles is always higher than samples continuously soaked into water. The reason for the trend in the strength development appears to be related hydrate generation accelerated during continuous D-W cycles. Figures 12(a), (b), and (c) show the relationships between the normalized cone index $q_c/(q_c)_{\text{continuous curing}}$ and t for thePSAS-N, PSAS-R, and BFCB-treated samples, respectively. Normalization was performed by dividing the q_c value of the sample by the (q_c) value of the sample continuously cured under soaked environment with the same t.

Figure 9 Appearance of sample after completing 4th D-W cycle

Table 4 Curing conditions for PSAS-N-treated, PSAS-R-treated, and BFCB-treated samples

Test scenario name			curing period under the soaked environment	Number of D-W cycles	Total curing period, (t)
PSAS-N-treated samples	PSAS-R-treated samples	BFCB-treated samples			
PSN-1	PSR-1	BFCB-1	1	Not applicable	1
PSN-3	PSR-3	BFCB-3	3	Not applicable	3
PSN-7	PSR-7	BFCB-7	7	Not applicable	7
PSN-14	PSR-14	BFCB-14	14	Not applicable	14
PSN-Cy-1	PSR-Cy-1	BFCB-Cy-1	Not applicable	1	3
PSN-Cy-2	PSR-Cy-2	BFCB-Cy-2	Not applicable	2	6
PSN-Cy-3	PSR-Cy-3	BFCB-Cy-3	Not applicable	3	9
PSN-Cy-4	PSR-Cy-4	BFCB-Cy-4	Not applicable	4	12

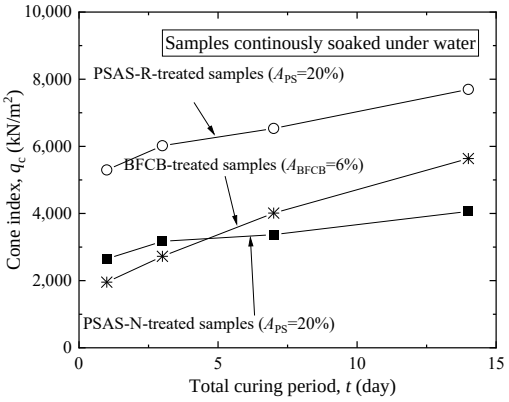

Figure 10 Relationships between the cone index (q_c) and total curing period (t) of the treated samples where sample was continuously soaked into water

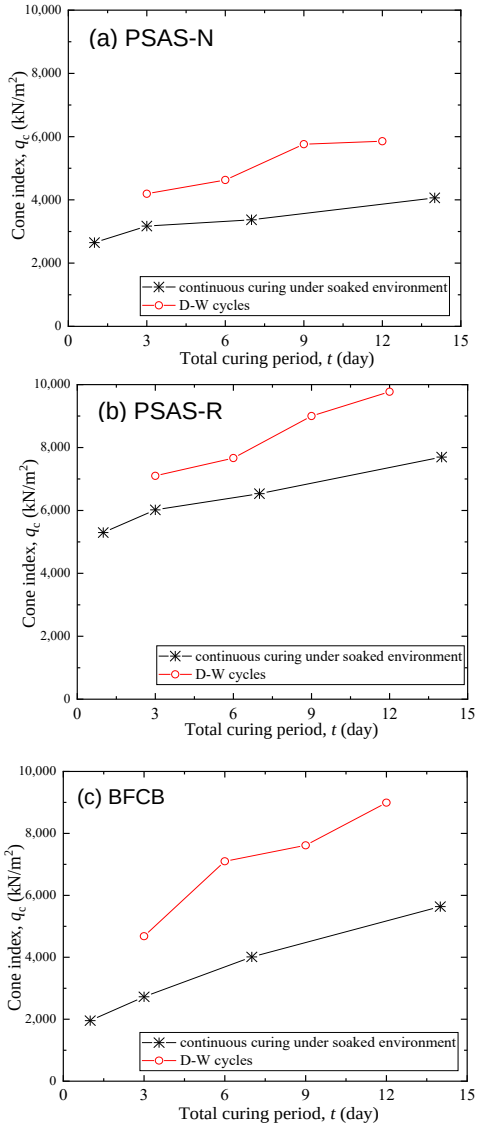

Figure 11 Relationships between q_c and t

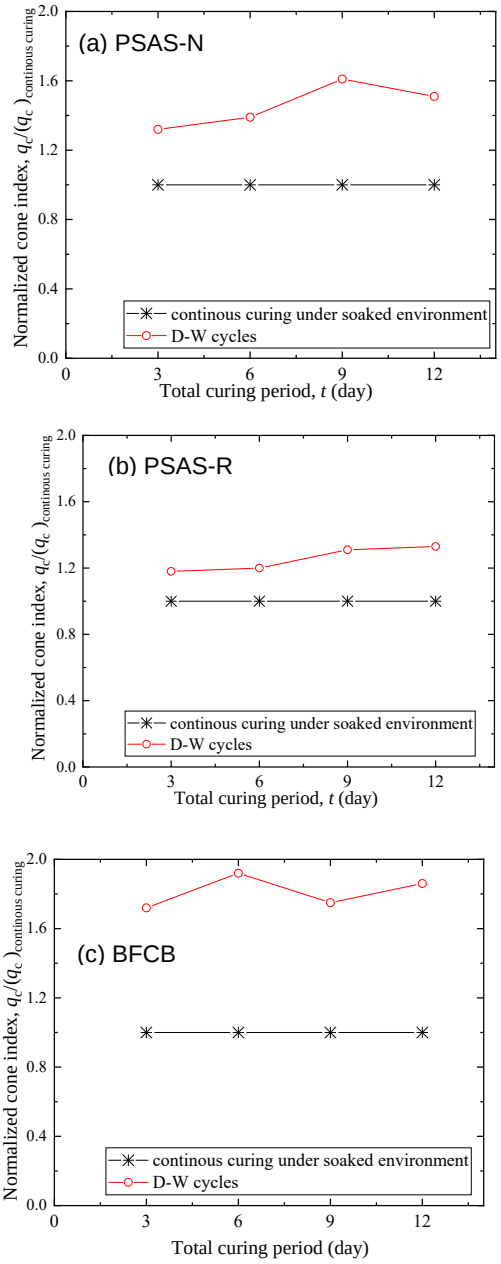

Figure 12 Relationships between the normalized cone index $(q_c/(q_c)_{continuous\ curing})$ and t

Due to repeated D-W cycles, q_c value of BFCB-treated samples increases from 72% to 92% whereas q_c value of PSAS-N-treated samples increases from 32% to 51%. PSAS-R-treated samples shows 18% to 33% strength increase. As mentioned earlier, the strength development of the BFCB- treated soils occurred through a hydration reaction, such as a pozzolanic reaction. For BFCB-treated samples, repeated D-W cycles accelerate generation of hydration. That's why BFCB-treated samples shows highest strength increase. On the other side, for the two PSASs, the excess water in the treated soil was physically absorbed by the porous structures of the PS ash particles and subsequently chemically used to generate hydrates during curing. For this reason, strength increase in PASAS-treated samples due to repeated D-W cycles is not that much high as BFCB-treated samples.

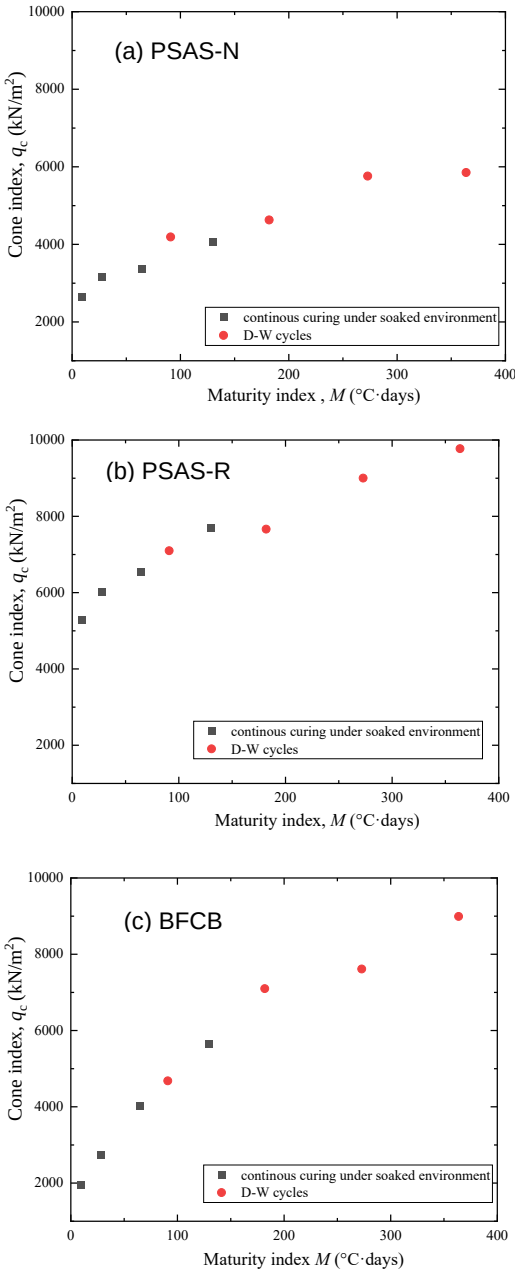

Figure 13 Influence of maturity index M_2 in q_c

In concrete engineering, several definitions of maturity index (M) is proposed by previous studies. Maturity is a concept that combines the effect of curing period and temperature. Following equations describes definition of maturity proposed by previous studies. (Kitazume et al., 2003).

$$M_1 = \Delta t * \sum_0^t (T - T_0) \quad [1.1]$$

$$M_2 = \Delta t * (2.1)^{(T-T_0)/10} \quad [1.2]$$

Here, M is maturity; T = Curing temperature; T_0 = Reference temperature (-10 °C); Δt = curing period (day).

Figure 13 (a), (b) (c) shows the relationship between the compressive strength and maturity index (M_2) in the PSAS-s and BFCB-treated specimens. A unique relationship between q_c and M_2 is observed. The maturity index clearly describes the strength development in PSAS-s and BFCB-treated specimens. With the increase in temperature, the strength of treated soil increases.

5. CONCLUSION

In this study, the effects of secondary curing conditions on the physical and strength characteristics of PSAS-treated soils were investigated using two types of PSASs with different water absorption and retention performances and then the result was compared with BFCB-treated soils. The experimental cone index test results revealed that the strength of treated samples continuously soaked into water is always lower than treated samples go through repeated D-W cycles regardless of the types of stabilizers. The strength development of the BFCB- treated soils occurred through a hydration reaction, such as a pozzolanic reaction. Repeated D-W cycles accelerates hydration reaction resulting strength increase. On the other hand, for the two PSASs, the excess water in the treated soil was physically absorbed by the porous structures of the PS ash particles and subsequently chemically used to generate hydrates during curing. Repeated D-W cycle in PSAS-s treated case cause hydrate generation though that might be different from those of cement treated sample. Further experiment is required to confirm whether the strength always increases with the progress of further D-W cycles and amount of drying process

6. REFERENCES

Djandjieme, M. O., Hayano, K., Yamauchi, H., and Maqsood, Z., 2022. Swelling and strength characteristics of sand treated with paper sludge ash-based stabilizer. Construction and Building Materials, 341, 127849.

Dong, P. H., Hayano, K., Kikuchi, Y., Takahashi, H., and Morikawa, Y., 2011. Deformation and crushing of particles of cement treat granulate soil. Soils and foundations, 51(4), 611-624.

Imai, K., Hayano, K., and Yamauchi, H., 2020. Fundamental study on the acceleration of the neutralization of alkaline construction sludge using a CO2 incubator. Soils and Foundations, 60(4), 800-810.

Inasaka, K., Trung, N. D., Hayano, K., and Yamauchi, H,. 2021. Evaluation of CO2 captured in alkaline construction sludge associated with pH neutralization. Soils and Foundations, 61(6), 1699-1707

Japanese Geotechnical Society. *Standards. JGS*, 0716, 2009: Test method for cone index of compacted soils. JGS, Tokyo, Japan.

Kitazume, M. and Satoh, T., 2003. Development of a pneumatic flow mixing method and its application to Central Japan International Airport construction. *Proceedings of the Institution of Civil Engineers-Ground Improvement*, *7*(3), pp.139-148.

Kitazume, M., Hayano, K., & Hashizume, H., 2003. Seismic stability of cement treated ground by tiltlng and dynamic shaklng table tests. Soils and foundations, 43(6), 125-140.

Kitazume, M. and Hayano, K., 2007. Strength properties and variance of cement-treated ground using the pneumatic flow mixing method. *Proceedings of the Institution of Civil Engineers-Ground Improvement*, *11*(1), pp.21-26.

Kawai, S., Hayano, K. and Yamauchi, H., 2018. Fundamental study on curing effect and its mechanism on the strength characteristics of PS ash-based improved soil. *Journal of Japan Society of Civil Engineers, Ser. C (Geosphere Engineering)*, *74*(3), pp.306-317.

Miyashita, Y., Sanjeewani, D. and Kuwano, R., 2019. Effect of curing conditions on long term mechanical property of improved surplus soils. In *E3S Web of Conferences* (Vol. 92, p. 11001). EDP Sciences.

Mochizuki, Y., Yoshino, H., Saito, E. and Ogata, T., 2003. Effects of soil improvement due to mixing with paper sludge ash. In *Proceeding of China-Japan Geotechnical Symposium* (pp. 1-8).

Phan, N.B., Hayano, K., Mochizuki, Y. and Yamauchi, H., 2021. Mixture design concept and mechanical characteristics of PS ash–cement-treated clay based on the water absorption and retention performance of PS ash. *Soils and Foundations*, *61*(3), pp.692-707.

Public Works Research Institute, 2013. Manual for utilization of soils from construction (4th edition). Public Works Research Center, 204.

Siham, K., Fabrice, B., Edine, A.N. and Patrick, D., 2008. Marine dredged sediments as new materials resource for road construction. *Waste management*, *28*(5), pp.919-928.

Trung, N.D., Ogasawara, T., Hayano, K. and Yamauchi, H., 2021. Accelerated carbonation of alkaline construction sludge by paper sludge ash-based stabilizer and carbon dioxide. *Soils and Foundations*, *61*(5), pp.1273-1286.

Watanabe, Y., Binh, P. N., Hayano, K., and Yamauchi, H., 2021. New mixture design approach to paper sludge ash-based stabilizers for treatment of potential irrigation earth dam materials with high water contents. Soils and Foundations, 61(5), 1370-1385.